

# DETERMINATION OF THE PITCH-ANGLE DISTRIBUTION AND TRANSVERSE ANISOTROPY OF INTERPLANETARY PARTICLES

C. K. Ng

Dept of Mathematics, University of Malaya  
Kuala Lumpur, Malaysia

**1. INTRODUCTION** We present a method to determine the directional differential intensity (d.d.i.), expressed in terms of spherical harmonics, from sectorized particle data, concurrent interplanetary magnetic field (IMF) and solar-wind velocity. In Section 2, we show the relation between the d.d.i. and the mean sector count rates  $X_1$ . In Section 3, we show how to estimate the d.d.i. from the measured  $X_1$  and the associated errors due to Poisson statistics. In Section 4, using the above method, we determine the pitch-angle distribution and the transverse anisotropy of the d.d.i. of low energy protons for the Day 118, 1978 solar particle event. In Section 5, we discuss an interesting correlation between the transverse anisotropy and the IMF direction.

## 2. RELATION BETWEEN DIRECTIONAL INTENSITY AND SECTOR RATES

We express the particle directional differential intensity as

$$j(p, \theta, \emptyset) = \sum_{n=0}^{\infty} \sum_{m=0}^n P_n^m(\cos \theta) \{ A_{nm}(p) \cos m\emptyset + B_{nm}(p) \sin m\emptyset \}, \quad (1)$$

where  $P_n^m$  = the associated Legendre functions,  $p$  = particle momentum,  $\theta$  = pitch-angle and  $\emptyset$  = gyrophase in the standard coordinate system (Ng, 1985). When the telescope points in the direction  $(\gamma, \eta)$ , it measures the differential count rates

$$C(p, \gamma, \eta) = \int_{\Omega} j(p, \theta, \emptyset) S[\theta'(\gamma, \eta, \theta, \emptyset)] \sin \theta d\theta d\emptyset, \quad (2)$$

where, following Sentman and Baker (unpublished manuscript), we express the angular response function of the particle telescope as

$$S(\theta') = \sum_{k=0}^{\infty} S_k P_k(\cos \theta') = \sum_{k=0}^{\infty} S_k \{ P_k(\cos \gamma) P_k(\cos \theta) + 2 \sum_{m=1}^k [(k-m)!/(k+m)!] P_k^m(\cos \gamma) P_k^m(\cos \theta) \cos m(\eta - \emptyset) \}. \quad (3)$$

It follows from the orthogonality of the spherical harmonics that

$$C(p, \gamma, \eta) = 4\pi \sum_{n=0}^{\infty} [S_n/(2n+1)] \sum_{m=0}^n \{ A_{nm}(p) \cos m\eta + B_{nm}(p) \sin m\eta \} P_n^m(\cos \gamma). \quad (4)$$

As the telescope sweeps over sector 1, we average (4) to obtain  $X_1(p)$  the mean differential count rate over sector 1,

$$X_1(p) = 4\pi \sum_{n=0}^{\infty} [S_n/(2n+1)] \sum_{m=0}^n \{ A_{nm}(p) \langle P_n^m(\cos \gamma) \cos m\eta \rangle_1 + B_{nm}(p) \langle P_n^m(\cos \gamma) \sin m\eta \rangle_1 \}, \quad (5)$$

where  $\langle \rangle_1 = (1/\Delta\psi) \int_{\psi_1}^{\psi_1+\Delta\psi} d\psi$ ,  $\psi$  = the spacecraft (s/c) spin-angle measured from the  $\psi_1$  projection of the IMF onto the spin plane, and  $(\psi_1, \psi_1+\Delta\psi)$  defines sector 1 (see the 2nd coordinate system in Fig. 1). For multiple-telescope systems (Sanderson & Hynds, 1977), eqn (5) should

be repeated for each telescope.

We now illustrate by specialising (1) and (5) to 8-sectored data for a telescope sweeping in the spacecraft's spin plane:

$$j(p, \theta, \varnothing) = \sum_{n=0}^4 A_{n0} P_n(\cos \theta) + \sum_{n=1}^3 A_{n1} P_n^1(\cos \theta) \cos \varnothing, \quad (6)$$

$$X_1 = 4\pi \sum_{n=0}^4 S_n A_{n0} Q_{n0}^1 / (2n+1) + 4\pi \sum_{n=1}^3 S_n A_{n1} Q_{n1}^1 / (2n+1), \quad (7)$$

$$\text{where } Q_{n0}^1 = \langle \sum_{j=0}^n a_j \sin^j \theta_B \cos^j \psi \rangle_1, \quad (8)$$

$$Q_{n1}^1 = \langle (\hat{W}_{11} \cos \psi + \hat{W}_{12} \sin \psi) \sum_{j=0}^n b_j \sin^j \theta_B \cos^j \psi \rangle_1, \quad (9)$$

$a_j$  = coefficient of  $x^j$  in  $P_n(x)$ ,  $b_j$  = coefficient of  $x^j$  in  $P_n^1(x)/(1-x^2)^{1/2}$ ,  $\theta_B$  = angle between IMF and s/c spin-axis, and  $(\hat{W}_{11}, \hat{W}_{12}, \hat{W}_{13})$  denotes a unit vector in the direction of  $\underline{E} \times \underline{B}$  in the 2nd coordinate system (Fig. 1). Note that the integrations in (8) and (9) may be performed readily in closed form.

**3. DETERMINATION OF  $j$  FROM MEASURED  $X_1$**  To simplify notation in the following, let

$$D_n = A_{n0} \quad (n=0,4), \quad D_n = A_{n-4,1} \quad (n=5,7), \quad (10)$$

$$R_n^1 = Q_{n0}^1 \quad (n=0,4), \quad R_n^1 = Q_{n-4,1}^1 \quad (n=5,7). \quad (11)$$

$$\text{We least-square fit } X_1 = \sum_{n=0}^7 C_n R_n^1, \quad (i=0,7), \quad (12)$$

to the 8 measured sector rates  $\bar{X}_1$ . This yields

$$\sum_{j=0}^7 H_{nj} C_j = \sum_{i=0}^7 R_n^1 \bar{X}_i, \quad (n=0,7), \quad (13)$$

$$\text{where } H_{nj} = \sum_i R_n^1 R_j^1, \quad (n=0,7; j=0,7). \quad (14)$$

Inverting (13), we have

$$C_n = \sum_k H_{nk}^{-1} \sum_i R_k^1 \bar{X}_i, \quad (n=0,7), \quad (15)$$

$$\text{and thence } D_n = \sum_i M_{ni} \bar{X}_i, \quad (n=0,7), \quad (16)$$

where  $M_{ni}$  is ultimately expressed in terms of  $Q_{n0}^1$ ,  $Q_{n1}^1$ , and  $S_n$ . Using (16), we may determine the coefficients  $A_{nm}$  in (6) by a matrix multiplication into the measured sector rates. When the IMF projection lies on a sector boundary, the symmetric matrix  $H_{nj}$  becomes singular. So we drop the  $A_{40}$  term in (6) whenever the IMF projection comes within  $2^\circ$  of a sector boundary.

Suppose that  $K_1$  counts are registered over the time interval  $t_c$  in sector 1. Assuming Poisson statistics, we estimate

$$X_1 = K_1/t_c, \quad \text{var}(X_1) = K_1/t_c^2, \quad \text{var}(D_n) = \sum_i M_{ni}^2 \text{var}(X_i). \quad (17)$$

If we define the anisotropy  $\xi_n = D_n/D_0$ , then, providing the counts are not too low,

$$\text{var}(\xi_n) \simeq (1/D_0^2) \sum_i (M_{ni} - \bar{\xi}_n M_{0i})^2 \text{var}(X_i). \quad (18)$$

Systematic errors are, of course, much harder to estimate.

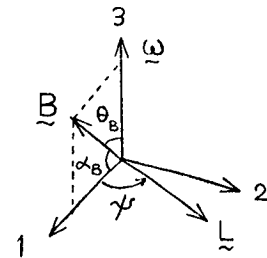


Fig. 1

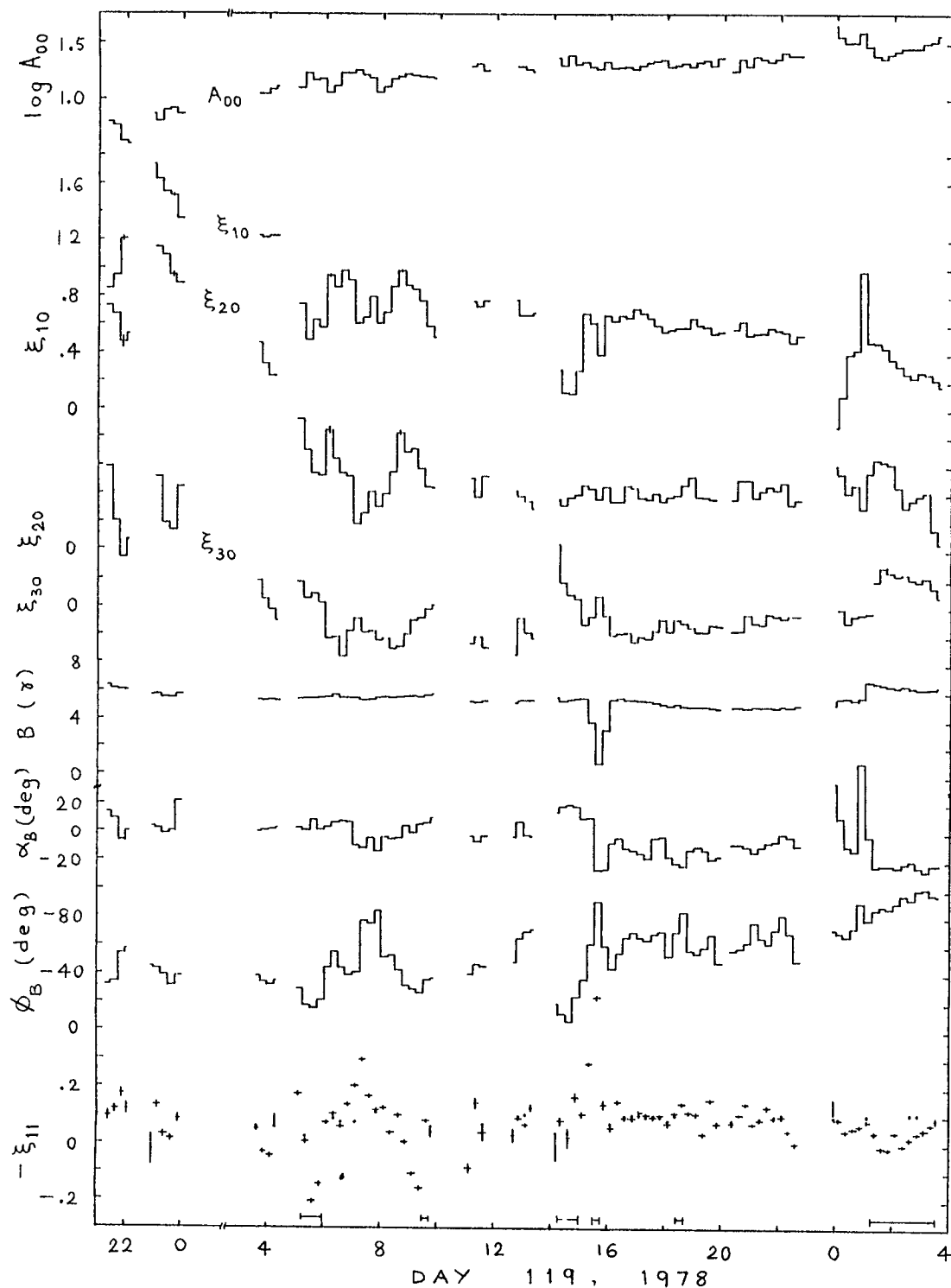


Fig. 2: 15-minute intensity and anisotropies of 1.4-2.5 MeV protons

4. APPLICATION As an example, we show in Fig. 2 the 15-min averages of  $A_{00}$ ,  $\xi_{10}$ ,  $\xi_{20}$ ,  $\xi_{30}$ , and  $-\xi_{11}$  for 1.4 - 2.5 MeV protons, determined

with the above method using 8-sectored particle data (P.I.: R.E. Vogt, CalTech), concurrent IMF (P.I.: N.F. Ness, GSFC), and hourly solar wind speed (P.I.: H. Bridge, MIT), measured aboard IMP-8 and accessed through NSSDC. Some typical standard errors due to Poisson statistics only are indicated by vertical bars.

Estimating the spectral slopes by using the corresponding results for 4-13 MeV protons, we have found the Compton-Getting corrections (Ng, 1985) for transformation to the  $\underline{ExB}$  drift frame to be small,  $<.002 A_{00}$ ,  $<.01$ ,  $<.01$ ,  $<.02$  for  $A_{00}$ ,  $\xi_{10}$ ,  $\xi_{20}$ , and  $\xi_{30}$  respectively. (For transformation to the solar wind frame, the corrections are of the order of  $0.04 A_{00}$ ,  $0.1$ ,  $0.3$ , and  $0.5$  respectively). Thus  $A_{00}$ ,  $\xi_{10}$ ,  $\xi_{20}$ ,  $\xi_{30}$  essentially characterise the pitch-angle distribution in the  $\underline{ExB}$  drift frame.

**5. DISCUSSION** The Compton-Getting correction,  $\varepsilon \hat{W}_1 (3 - pA_{20}/A_{00} + pA_{20}/5A_{00})$  to the transverse anisotropy  $-\xi_{11}$  is indicated by the dots in Fig. 2. The observed anisotropy varies in phase with this correction but is much larger in magnitude. The same feature, even more marked, is seen for 4-13 MeV protons. What is the cause of this large discrepancy?

For Fig. 2, IMP-8's GSE coordinates in  $R_E$  varies from (21.6, 21.5, 5.5) to (5.7, 29.5, 18.1). The times when the IMF is connected to the nominal bow shock (BS) are indicated by horizontal bars in Fig. 2 (Ng & Roelof, 1977). At ~1537 UT Day 119, some solar particles with guiding centres below the IMF through IMP-8 are probably shadowed by the nose of the BS, resulting in the observed peak value of  $-\xi_{11} = 0.53$ . However BS connection does not account for the general variation of  $-\xi_{11}$  in Fig. 2.

Close inspection reveals that the sector plot of  $X_1$  lags behind the IMF in directional changes. Hence a tentative explanation is that some observed 15-min averages contain a substantial fraction of non-gyrotropic distributions which reside a short distance ( $\sim 1$  gyroradius) beyond a 'kink' in the IMF. An alternative explanation is as follows. When  $\theta_B$  swings rapidly in an averaging interval such that its average value is close to one end of the range of values, then a field-aligned anisotropy  $\xi_{10}$  would "induce" a nonzero value of  $-\xi_{11}$ , i.e., the apparent value of  $-\xi_{11}$  is not real. Further studies with smaller averaging intervals would clarify this matter.

**6. CONCLUSION** We have shown how to obtain the directional differential intensity referred to the standard coordinate system (Ng, 1985) from sectored particle data and concurrent IMF and solar wind data. The corrections for transformation to the  $\underline{ExB}$  drift frame are explicitly calculated and found to be small for these  $\sim 1.5$  MeV protons. However, the new correction formulae would be important for  $\lesssim 500$  KeV protons. It is tentatively suggested that the 'observed' transverse anisotropy may in large part be induced by a rapidly changing IMF in the presence of a field-aligned anisotropy.

**Acknowledgement** Prof E.C. Stone's hospitality and the advice of Drs. R.A. Mewaldt and T.G. Garrad on CalTech EIS experiment are gratefully acknowledged. I thank B.L. Ng for helping to prepare the manuscript.

## References

- Ng, C.K. (1985) Paper SH 3.1-10, this conference.
- Sanderson, T.R. & Hynds, R.J. (1977) *Planet. Space Sci.*, 25, 799.
- Ng, C.K. & Roelof, E.C. (1977) *EOS Trans. A.G.U.*, 58, 1205.